Haptic Manipulation of Virtual Linkages with Kinematic Loops

M. Beenakkers and D. Constantinescu and M. Steinbuch

***Abstract*— This paper proposes an approach to providing realistic force feedback to users manipulating virtual linkages with kinematic loops. In the proposed approach, users feel the effect of the effect of the virtual kinematic loops: (a) on the inertia of the virtual linkage at the user-selected operational point (OP); and (b) on their freedom of motion. The approach introduces a method for computing the inertia of linkages with kinematic loops at arbitrarily selected OPs. It uses this inertia to select the directions of motion resisted by the virtual joints. Users feel the apparent inertia via impedance control, and the motion restrictions via stiffness control. Controlled experiments within a planar haptic interaction system validate that the proposed approach successfully renders the kinematic loop closure constraints to users.**

I. Introduction

Haptics applications strive to provide force feedback to users interacting with realistic virtual environments (VEs). A key factor affecting the realism of the VE is the complexity of the virtual objects that users can manipulate (hereafter called virtual tools, VTs). VT complexity is typically limited by the stringent speed requirements of the haptic controller. For compelling interaction within rigid VEs, the haptic controller demands the VT dynamics to be computed at guaranteed rates of the order of hundreds of Hz. Many haptics applications meet these severe control constraints through enabling users to manipulate only single virtual objects.

More complex VTs may be needed in various applications. For example, during virtual reality-based training for robot assisted minimally invasive surgery, surgeons need to manipulate VTs with motion constrained by the robotic system. Virtual CAD prototyping and animation applications may also require users to operate virtual linkages. In contrast to the manipulation of single objects, force interaction with virtual linkages commands the haptic rendering of the linkage dynamics, including the varying inertia and the joint constraints.

Earlier haptics work has proposed linkage simulations that run at the speed of the haptic controller. Computational efficiency has been achieved via application-specific [14] and general purpose algorithms [17], [19]. More recently, a multi-rate architecture has been proposed whereby linkage dynamics are simulated in minimal coordinates at the speed of the haptic controller [10], [11]. The efficient dynamics in minimal coordinates are obtained via symbolic constraint embedding performed outside the main integration loop. It is envisioned that computational power increases will soon allow the use of this architecture in haptic applications. Increased physical accuracy of the haptic simulation of linkages has also been sought via modeling collisions in [18], [3]. The haptic rendering of the joint constraints of serial-chain VTs has been implemented via proxies with first order dynamics in [13] and via a controller acting along the constrained directions in [5]. Apart from the haptic manipulation of a VT with a kinematic loop reported in [14] and based on an application-specific simulation and haptic rendering algortihm, mostly haptic interaction with serial-chain VTs has been investigated to date.

The present work expends the class of VTs that users can manipulate to include passive linkages with kinematic loops (linkages under feedback control, i.e., active, can also be included in the proposed formulation). It enables users to feel the VT inertia and the motion restrictions due to the kinematic loops. The work contributes a technique for computing the inertia of VTs with kinematic loops at an arbitrary OP, and for deriving the motion constraints imposed on users by the virtual joints. The VT inertia is applied to users via impedance control. The directions of constraint are rendered via stiffness control. As illustrated in Section VI, stiffness control effectively restricts users' motion as required by the kinematic loops.

In the remainder, the simulation of VTs with kinematic loops enforced via Lagrange multipliers is briefly discussed in Section II. The haptic rendering of the dynamics of VTs with kinematic loops is overviewed in Section III. The derivation of the VT inertia and of the kinematic loop closure constraints at the user-selected OP is developed in Section IV. The efficient implementation of the approach is detailed in Section V. Haptic manipulation of a VT with kinematic loops is illustrated in Section VI. Concluding remarks are presented in Section VII.

II. Linkage Simulation

VTs with kinematic loops are simulated in the present work through the method of Lagrange multipliers in its form common in multibody dynamics [15], [16], [9]. Specifically, the VT dynamics are derived using extended generalized coordinates [6]. These coordinates include the relative joint coordinates identified after selecting cut joints and cutting them open, as illustrated in Fig. 1 for a VT with one kinematic loop. Note that the selection of the cut joints is beyond the scope of the present work, and has no bearing on the proposed algorithm for haptic rendering of kinematic

M. Beenakkers and M. Steinbuch are with the Department og Mechanical ENgineering, Eindhoven University of Technology, Eindhoven, The Netherlands m.a.beenakkers@student.tue.nl, m.steinbuch@tue.nl

D. Constantinescu is with the Department of Mechanical ENgineering, University of Victoria, Victoria, Canada danielac@me.uvic.ca

loops because the VT dynamics are independent of this selection.

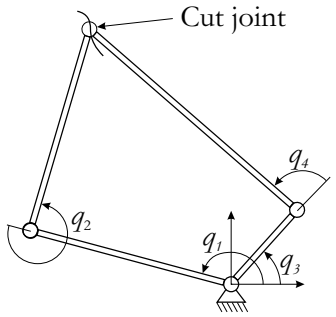

Fig. 1. Choice of configuration variables for a VT with kinematic loops.

In the chosen (dependent) configuration variables, the dynamics of a VT with n links, m kinematic loop closure constraints and c contacts are given by:

$$\mathbf{D}\left(\mathbf{q}\right)\ddot{\mathbf{q}} + \mathbf{B}\left(\mathbf{q},\dot{\mathbf{q}}\right) + \mathbf{G}\left(\mathbf{q}\right) = \sum_{i=1}^{c} \mathbf{J}_i^T\left(\mathbf{q}\right)\mathbf{F}_i + \mathbf{J}_h^T\left(\mathbf{q}\right)\mathbf{F}_h - \mathbf{W}^T\left(\mathbf{q}\right)\boldsymbol{\lambda}, \quad (1)$$

where: $\mathbf{D}\left(\mathbf{q}\right)_{n\times n}$ is the configuration space mass (inertia) matrix of the VT; $\mathbf{B}\left(\mathbf{q},\dot{\mathbf{q}}\right)_{n\times 1}$ groups Coriolis and centripetal terms; $\mathbf{G}\left(\mathbf{q}\right)_{n\times 1}$ encompasses joint flexibility and gravitational effects; $\mathbf{J}_i\left(\mathbf{q}\right)_{6\times n}$ is the linkage Jacobian computed at the i-th contact; $\mathbf{F}_{i_{6\times 1}} = \begin{pmatrix}\mathbf{f}_i^T & \mathbf{0}^T\end{pmatrix}^T$ is the contact wrench (i.e., the force $\mathbf{f}_{i_{3\times 1}}$ and torque $\boldsymbol{\tau}_{i_{3\times 1}} = \mathbf{0}_{3\times 1}$) at the i-th contact; $\mathbf{J}_h\left(\mathbf{q}\right)_{6\times n}$ is the VT Jacobian computed at the user's hand (hand Jacobian); $\mathbf{F}_{h_{6\times 1}}$ is the wrench applied by the user; $\mathbf{W}\left(\mathbf{q}\right)_{m\times n} = \frac{\partial \mathbf{h}(\mathbf{q})}{\partial \mathbf{q}}$ is the rectangular Jacobian of the kinematic loop closure constraints; $\boldsymbol{\lambda}_{m\times 1}$ is the vector of Lagrange multipliers, i.e., unknown magnitudes of constraint forces maintaining the closed loops at the cut joints; and $\mathbf{q}_{n\times 1}$, $\dot{\mathbf{q}}_{n\times 1}$, and $\ddot{\mathbf{q}}_{n\times 1}$ are the configuration space position, velocity, and acceleration of the VT, respectively. (1) describes the dynamics of a passive VT. Haptic manipulation of VTs under feedback control (i.e., active) can be allowed by augmenting (1) with the desired feedback torques.

Integration of a DAE of index three [2] is avoided through augmenting the VT dynamics in (1) with acceleration constraints. For the holonomic constraints considered here, the acceleration constraints result from differentiating the kinematic loop closure constraints $\mathbf{h}\left(\mathbf{q}\right)_{m\times 1} = 0$ twice to obtain:

$$\ddot{\mathbf{h}} = \mathbf{W}\ddot{\mathbf{q}} + \mathbf{w} = \mathbf{0}. \quad (2)$$

In (2), $\mathbf{w} = \left(\frac{\partial \mathbf{W}}{\partial t} + \frac{\partial \mathbf{W}}{\partial \mathbf{q}}\dot{\mathbf{q}}\right)\cdot\dot{\mathbf{q}}$ and the dependence of the various terms on $\dot{\mathbf{q}}$, $\mathbf{q}$, and time t is implied. Kinematic loop closure drift is kept small through Baumgarte stabilization [1], i.e., through replacing (2) with:

$$\ddot{\mathbf{h}} + 2\alpha\beta\dot{\mathbf{h}} + \alpha^2\mathbf{h} = 0 \Leftrightarrow \mathbf{W}\ddot{\mathbf{q}} + \mathbf{w}_{stab} = \mathbf{0}. \quad (3)$$

In (3), $\mathbf{w}_{stab} = \mathbf{w} + 2\alpha\beta\mathbf{W} + \alpha^2\mathbf{h}$, and α and β are chosen such that the error dynamics converge to zero.

After augmenting the VT dynamics with the Baumgarte stabilized loop closure constraints at the acceleration level, the haptic simulation solves:

$$\begin{bmatrix}\mathbf{D} & \mathbf{W}^T\\ \mathbf{W} & \mathbf{0}\end{bmatrix}\begin{pmatrix}\ddot{\mathbf{q}}\\ \boldsymbol{\lambda}\end{pmatrix} = \begin{pmatrix}\sum_{i=1}^{c}\mathbf{J}_i^T\mathbf{F}_i + \mathbf{J}_h^T\mathbf{F}_h - \mathbf{B} - \mathbf{G}\\ -\mathbf{w}_{stab}\end{pmatrix} \quad (4)$$

and integrates the configuration acceleration in fixed steps equal to the time step of the force feedback loop. For non-redundant kinematic loop closure constraints, $\mathbf{W}$ is non-singular and the computational delay inccured through solving $n+m$ ODEs in the proposed approach, compared to $n-m$ ODEs in methods which derive the VT dynamics in independent coordinates, is minor for VTs with a limited number of kinematic loops. This cost is partly offset through avoiding the need to identify new sets of configuration variables during the simulation, as would be necessary if minimal coordinates would be used. Another advantage of enforcing the loop closure constraints through Lagrange multipliers is that techniques are available for efficiently deriving the Lagrangian dynamics of multibody systems with tree kinematic structures [7].

III. Haptic Rendering of Linkage Dynamics

During manipulation of VTs with kinematic loops, users need to feel: (i) the inertia of the VT at the selected OP; (ii) the virtual joints when attempting to move outside the space of feasible motions and (iii) the contacts of the VT when other virtual objects restrict the VT motion. The present work employs a control architecture whereby separate controllers render inertia, joint constraints and contacts to users [5]. This control architecture, schematically depicted in Fig. 2, includes the following controllers:

1) *Impedance controller*: renders the VT dynamics during free motion of the user-selected OP (i.e., motion unimpeded by the joints or other objects). Based on the inverse of the VT operational space inertia $\boldsymbol{\Lambda}_h^{-1}$, this controller shapes the impedance of the device to match the VT impedance at the OP.
2) *Joint constraint controller*: renders the resistance of the virtual joints when users try to move outside the space of feasible operational space motions. This is a stiffness controller which hinders motion along the directions $\mathbf{n}_c$ resisted by the virtual joints.
3) *Four channel teleoperation controller* [12]: renders the VT contacts through feedforwarding the hand $\mathbf{F}_h$ and contact $\mathbf{F}_i$ wrenches between the haptic device (user) and the haptics simulation via the two force channels. It eliminates user's drift from the OP via the two position channels.

To enable manipulations of VTs with kinematic loops, this architecture requires the VT inertia and the directions resisted by the cut joints at the selected OP. A method for computing them is proposed in the following section.

IV. Linkage inertia at the operational point

In contrast to serial-chain VTs with dynamics in independent coordinates, the dynamics of VTs with kinematic

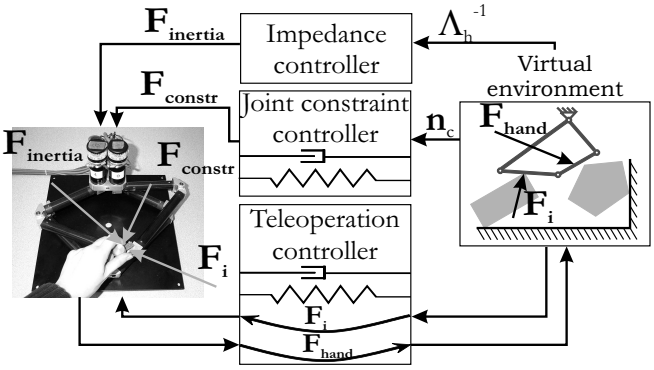

Fig. 2. Schematic of the control architecture rendering the VT dynamics.

loops are simulated in extended generalized coordinates and the loop closure constraints are included via Lagrange multipliers. Therefore, users must perceive the effect of the Lagrange multipliers on the VT operational space dynamics in addition to feeling the VT contacts. While the contact wrenches $\mathbf{F}_i$ between the VT and other virtual objects are computed using impulsive and penalty forces as proposed in [3], the effect of the Lagrange multipliers is derived herein under the simplifying assumption of small velocities, i.e., neglijible dynamic coupling effects. The validity of this assumption is verified experimentally in Section VI.

Given the assumption of small velocities, the operational space acceleration of the user's hand is [8]:

$$\ddot{\mathbf{x}}_h = \mathbf{J}_h \ddot{\mathbf{q}} = \mathbf{\Lambda}_h^{-1} \mathbf{F}_h, \tag{5}$$

where $\mathbf{\Lambda}_h^{-1}$ is the inverse of the VT operational space inertia at the selected OP. Note in (5) that the space of feasible motions at the OP can be identified with the range space of $\mathbf{\Lambda}_h^{-1}$, and the space of user motions hindered by the virtual joints can be identified with the null space of $\mathbf{\Lambda}_h^{-1}$. Substituting $\ddot{\mathbf{q}}$ from (1) in (5), it follows that:

$$\mathbf{\Lambda}_h^{-1} \mathbf{F}_h = \mathbf{J}_h \mathbf{D}^{-1} \left(\mathbf{J}_h^T \mathbf{F}_h - \mathbf{W}^T \boldsymbol{\lambda} \right), \tag{6}$$

where $\mathbf{\Lambda}_h^{-1}$ and $\boldsymbol{\lambda}$ are unknown. Therefore, the constraint equation (2) is used to compute the Lagrange multipliers:

$$\boldsymbol{\lambda} = - \left(\mathbf{W} \mathbf{D}^{-1} \mathbf{W}^T \right)^{-1} \mathbf{W} \mathbf{D}^{-1} \mathbf{J}_h^T \mathbf{F}_h. \tag{7}$$

Substitution of (7) into (6) gives:

$$\mathbf{\Lambda}_h^{-1} \mathbf{F}_h = \mathbf{J}_h \mathbf{D}^{-1} \left(\mathbf{J}_h^T - \mathbf{W}^T \left(\mathbf{W} \mathbf{D}^{-1} \mathbf{W}^T \right)^{-1} \mathbf{W} \mathbf{D}^{-1} \mathbf{J}_h^T \right) \mathbf{F}_h. \tag{8}$$

which must hold for all hand wrenches $\mathbf{F}_h$. Hence:

$$\begin{aligned} \mathbf{\Lambda}_h^{-1} &= \mathbf{J}_h \mathbf{D}^{-1} \left(\mathbf{J}_h^T - \mathbf{W}^T \left(\mathbf{W} \mathbf{D}^{-1} \mathbf{W}^T \right)^{-1} \mathbf{W} \mathbf{D}^{-1} \mathbf{J}_h^T \right) \\ &= \mathbf{J}_h \mathbf{D}^{-1} \mathbf{J}_h^T - \mathbf{J}_h \mathbf{D}^{-1} \mathbf{W}^T \left(\mathbf{W} \mathbf{D}^{-1} \mathbf{W}^T \right)^{-1} \mathbf{W} \mathbf{D}^{-1} \mathbf{J}_h^T. \end{aligned} \tag{9}$$

In (9), the first term is the inverse of the operational space inertia of the VT with the kinematic loops opened and the second term embeds the kinematic loop closure effects. Note the coupling between loop closure geometry and configuration space inertia for VTs with dynamics in extended generalized coordinates. Due to this coupling, the kinematic loop closure constraints are computed in this work alongside the other joint constraints via singular value decomposition (SVD) of $\mathbf{\Lambda}_h^{-1}$:

$$\mathbf{\Lambda}_h^{-1} = \mathbf{U} \mathbf{\Sigma} \mathbf{V}^T. \tag{10}$$

Specifically, the directions of joint constraints, including the cut joint constraints, form the rows of $\mathbf{U}$.

V. Implementation

Because SVD algorithms do not have guaranteed running time, the computation of the singular directions of $\mathbf{\Lambda}_h^{-1}$ is sidestepped in the proposed implementation via decoupling the force control loop from the simulation through a local model of interaction [4] (see Fig. 3). The local model is a reduced simulation that runs at the frequency of the force control loop. It approximates the interaction between the VT and the VE through the interaction between the VT and nearby objects. The approximate dynamic model of the VT employed in the local model is called the dynamic proxy. The quality of the approximation is maintained via updating the local model at each step of the VE simulation.

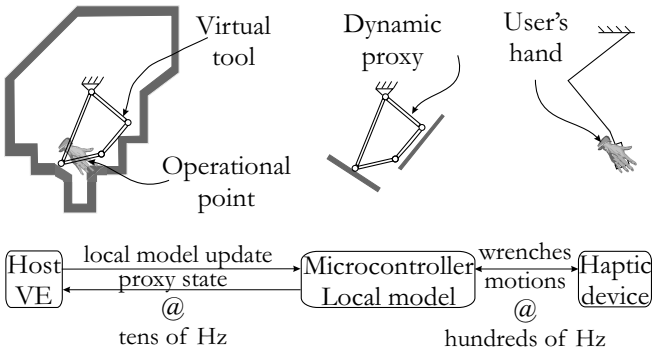

Fig. 3. Decoupling of the force control loop from the VE simulation through a local model of interaction.

The decoupling permits computations to be distributed between the simulation/graphics and the haptics processors. Specifically, contact geometry, $\mathbf{\Lambda}_h^{-1}$ and the directions of joint constraint are computed on the graphics processor. The VT dynamics are computed on the haptics processor and are rendered to users as described in Section III. Further computational savings are achieved on the haptics processor by approximating $\mathbf{D}$, $\mathbf{W}$, and $\mathbf{w}$ in (4) with their values in the VE at the moment of the update. Lastly, it is assumed that users manipulate the VT slow enough that the Coriolis and centripetal effects can be ignored (similar to work in [17] and [19]) and the VT dynamics are simulated by:

$$\begin{bmatrix} \widehat{\mathbf{D}} & \widehat{\mathbf{W}}^T \\ \widehat{\mathbf{W}} & \mathbf{0} \end{bmatrix} \begin{pmatrix} \ddot{\mathbf{q}} \\ \boldsymbol{\lambda} \end{pmatrix} = \begin{pmatrix} \sum_{i=1}^{c} \mathbf{J}_i^T \mathbf{F}_i + \mathbf{J}_h^T \mathbf{F}_h - \widehat{\mathbf{G}} \\ -\widehat{\mathbf{w}}_{stab} \end{pmatrix} \tag{11}$$

In (11), $\widehat{\mathbf{D}}$, $\widehat{\mathbf{W}}$, $\widehat{\mathbf{w}}_{stab}$ and $\widehat{\mathbf{G}}$ denote the values of $\mathbf{D}$, $\mathbf{W}$, $\mathbf{w}_{stab}$ and $\mathbf{G}$, respectively, computed by the graphics engine and sent to the local model at the update. Furthermore, the directions of joint constraint are approximated through their

values in the VE at the update, by computing the SVD of $\mathbf{\Lambda}_h^{-1}$ on the graphics processor:

$$\widehat{\mathbf{\Lambda}}_h^{-1} = \widehat{\mathbf{U}}\widehat{\mathbf{\Sigma}}\widehat{\mathbf{V}}^T \tag{12}$$

and using the columns of $\widehat{\mathbf{U}}$ in the local model to estimate these directions. Equations (11) and (12) allow the VT dynamics to be simulated at the frequency of the haptic controller. Operation of VTs with kinematic loops using these approximations is demonstrated experimentally in the following section.

The block diagram of the user manipulation of the dynamic proxy of a VT with kinematic loops in a free VE ($\mathbf{F}_i = \mathbf{0}$) is depicted in Fig. 4. This figure represents: the user through the hand wrench $\mathbf{F}_h$; the joint constraint controller that limits user's motion as required by the kinematic loops through its stiffness k_j and damping b_j; and the four channel teleoperation controller through the force channels feedforwarding the hand wrench $\mathbf{F}_h$ to the local model, and through the stiffness $\mathbf{K}_{pc}$ and damping $\mathbf{B}_{pc}$ of its position channels.

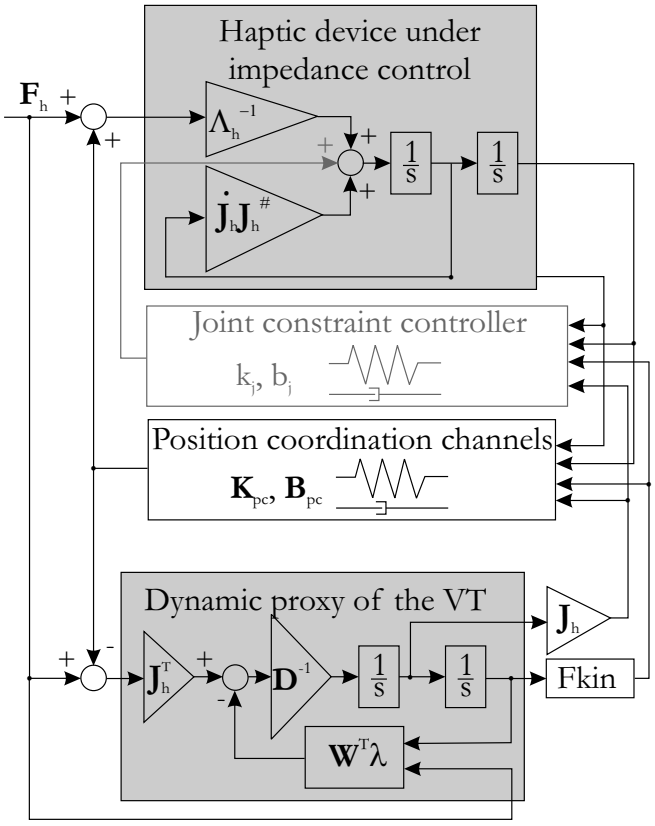

Fig. 4. Block diagram of the manipulation of a VT with kinematic loops in a free VE. User motion along the directions resisted by the loop closure constraints has stiffness k_j and damping b_j.

VI. Experiments

This section illustrates manipulations of the VT depicted in Fig. 5, whose parameters are given in Table I. A controlled constant wrench $\mathbf{F}_h = \begin{pmatrix}-0.5\text{N} & 0\text{N} & -0.0025\text{Nm}\end{pmatrix}^T$[1] is applied at the centre of mass of the second link in the experiment (note link numbering in Fig. 5). This constant wrench ensures the "same" user during successive manipulations. The VT is initially at rest in the position $\mathbf{q}_0 = \begin{pmatrix}\frac{\pi}{4}\text{rad} & -\frac{\pi}{2}\text{rad} & -\frac{4\pi}{10}\text{rad} & \frac{\pi}{2}\text{rad}\end{pmatrix}^T$, as depicted in Fig. 5. The stiffness and damping used for rendering joint constraints are $k_j = 200$N/m/kg and $b_j = 50$N/(m/s)/kg. Kinematic correspondence between the device and the VT are maintained via $\mathbf{K}_{pc} = \begin{pmatrix}100\text{N/m} & 100\text{N/m} & 0.5\text{Nm/rad}\end{pmatrix}^T$ and $\mathbf{B}_{pc} = \begin{pmatrix}70\text{N/(m/s)} & 70\text{N/(m/s)} & 0.375\text{Nm/(rad/s)}\end{pmatrix}^T$. These gains are chosen to be much weaker than the contact stiffness and damping, implemented in the haptic simulation via $k_{contact} = 15,000$Nm and $b_{contact} = 300$N/(m/s). The gains of the graphics controller are $\mathbf{K}_g = \begin{pmatrix}1000\text{N/m} & 1000\text{N/m} & 100000\text{Nm/rad}\end{pmatrix}^T$ and $\mathbf{B}_g = \begin{pmatrix}100\text{N/(m/s)} & 100\text{N/(m/s)} & 10000\text{Nm/(rad/s)}\end{pmatrix}^T$. These are the maximum values for which the VE simulation on the graphics processor is stable. Because the testbed VE includes only the VT, its dynamics are approximated by:

$$\widehat{\mathbf{D}}\ddot{\mathbf{q}} = \mathbf{J}_h^T\mathbf{F}_h - \widehat{\mathbf{W}}^T\boldsymbol{\lambda} \tag{13}$$

in the local model of interaction.

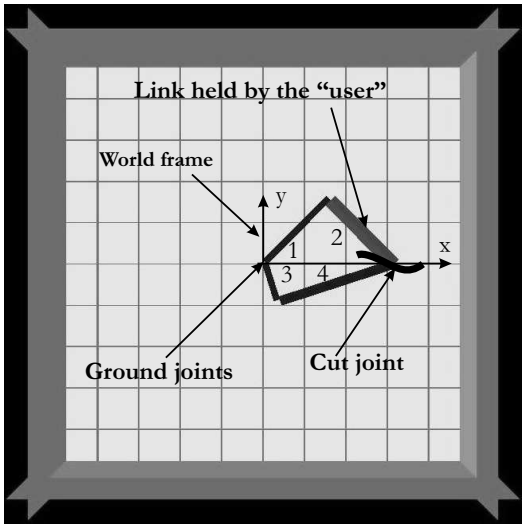

Fig. 5. Planar testbed virtual environment used to illustrate haptic manipulation of VTs with kinematic loops. Note link numbering and the cut joint.

TABLE I
VT parameters in the experimental manipulations.

Link length	Link mass	Link inertia
$l_1 = 0.045$ (m)	$m_1 = 1$ (kg)	$I_1 = 0.0021$ (kg·m^2)
$l_2 = 0.045$ (m)	$m_2 = 1$ (kg)	$I_2 = 0.0021$ (kg·m^2)
$l_3 = 0.021$ (m)	$m_3 = 1$ (kg)	$I_3 = 0.0021$ (kg·m^2)
$l_4 = 0.060$ (m)	$m_1 = 0.5$ (kg)	$I_1 = 0.00105$ (kg·m^2)

The proposed method for computing $\mathbf{\Lambda}_h^{-1}$ and the directions of kinematic loop closure constraint is validated via

[1]For the impedance type haptic interface used in the experiment, a constant wrench is a worst case approximation of the user for stability.

two successive manipulations. During the first manipulation, the loop closure constraint is imposed through stiffness control by penalizing motion along the directions resisted by the cut joint. During the second manipulation, the loop closure costraint is rendered through impedance control by controlling the acceleration of the end-effector of the haptic device to zero along the directions of cut joint constraint. The experimental results are plotted in Figs. 6 and 7. Figs. 6(a) and 7(a) depict the number of joint constraints imposed on the haptic device (i.e., the user's hand) by the VT, identifying the time during which the loop closure constraint is active in each manipulation. They illustrate that, in the VE, the virtual joints impose at least one constraint on the OP throughout both manipulations. This is because the selected OP is on a link with insufficient degrees of freedom. Hence, during either manipulation, the loop closure constraint is active ($\lambda \neq 0$) only when two joint constraints are active in the haptic simulation.

Figs. 6(b) and 7(b) plot the trajectories of the end-effector of the haptic device (HD) and of the selected OP on the VT (OP). Although the different controllers change the VT dynamics and thus the OP trajectories during the two manipulations, a qualitative comparison of the results is possible. Note that the trajectory of the end-effector of the haptic interface follows the trajectory of the simulated OP when joint constraints are rendered via stiffness control (Fig. 6(b)). In contrast, the drift between the two trajectories is significant when joint constraints are imposed via impedance control (Fig. 7(b))[2]. These results illustrate that stiffness control enforces the cut joint as effectively as the serial-chain joint. Hence, they validate the method proposed for computing $\mathbf{\Lambda}_h^{-1}$ and the kinematic loop closure constraint directions. The effect of the loop closure constraint on the device (i.e., on the user) motion is also clearly identifiable in Fig. 6(c). Note in this figure that the wrench applying the joint constraints to the device (hand) is larger when the kinematic loop closure constraint is active. This larger wrench demonstrates that the stiffness of the two constraints combines to tighter confine the device to the simulated OP.

VII. Conclusion

This paper has proposed an approach to enabling users to manipulate virtual linkages with kinematic loops. In this approach, linkage dynamics are simulated in configuration space and kinematic loop closure constraints are maintained via Lagrange multipliers augmented with Baumgarte stabilization terms. The virtual dynamics are rendered to users in Cartesian space. The varying linkage inertia is applied via impedance control in operational space, and the joint contraints are enforced via stiffness control along directions orthogonal to operational space. The ability to restrict user's motion as required by the virtual kinematic loops has been validated through an experiment within a planar haptic interaction system.

[2]The drift in Fig. 7(b) is limited by ending the experiment before the device end-effector reaches the mechanical boundary of its workspace, after approximately 3s and just after the loop closure constraint becomes active.

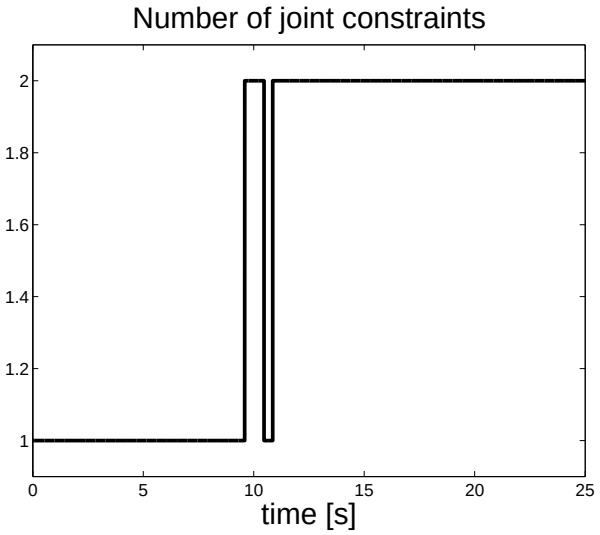

(a) Number of joint constraints imposed by the VT on the OP.

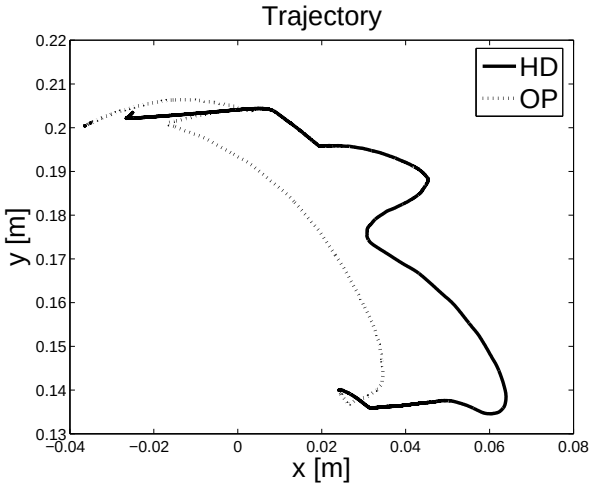

(b) Experimental trajectories: of the user's hand on the haptic device (HD); and of the OP on the VT (OP).

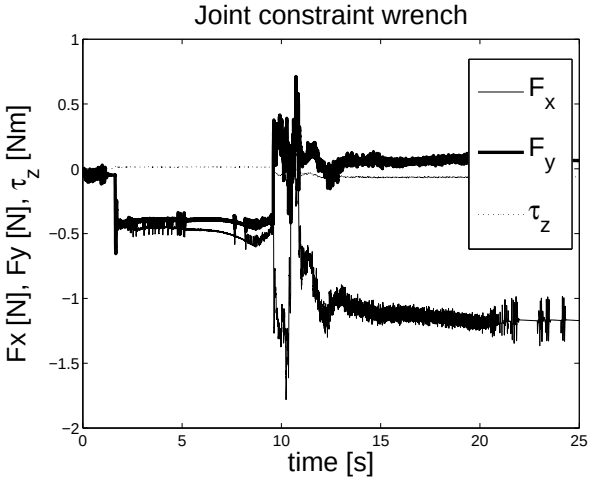

(c) Joint constraint wrench applied to the user's hand by the stiffness controller on the haptic device and the OP on the VT.

Fig. 6. Experiment: joint constraints rendered through stiffness control.

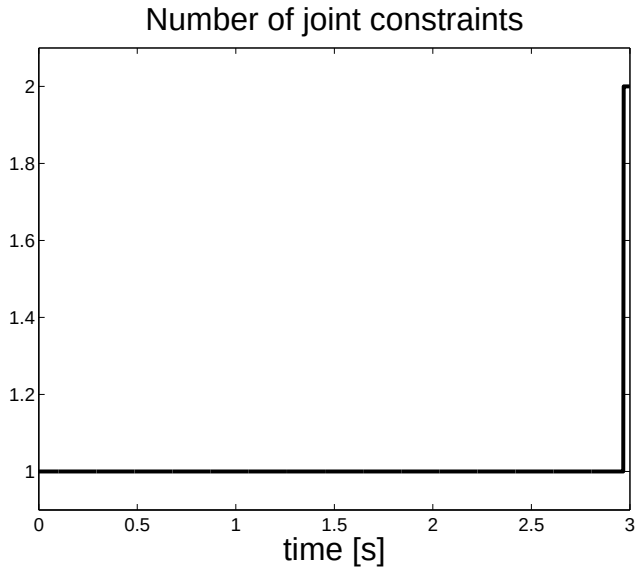

(a) Number of joint constraints imposed by the VT on the OP.

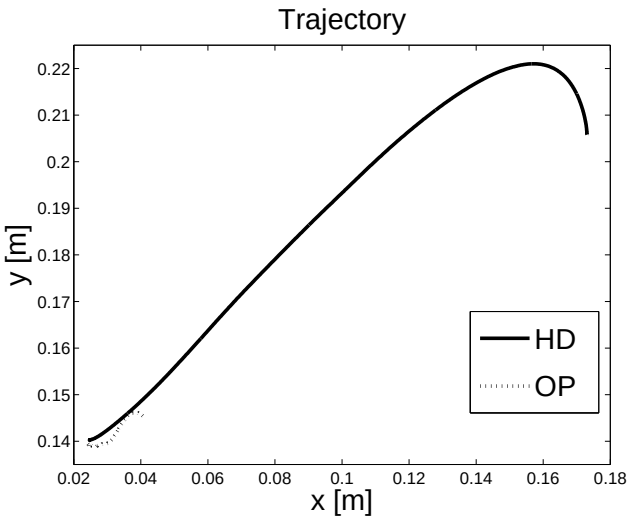

(b) Experimental trajectories: of the user's hand on the haptic device (HD); and of the OP on the VT (OP).

Fig. 7. Experiment: joint constraints rendered through impedance control.

Future work will investigate: the range of stiffness controller gains for guaranteed stable manipulation of VTs with kinematic loops; the haptic manipulation of active VTs, i.e., VTs under feedback control; the operation of VTs with redundant loop closure constraints; and the simultaneous manipulation of a VT with kinematic loops by multiple users.

REFERENCES

[1] J. Baumgarte, "Stabilization of Constraints and Integrals of Motion in Dynamical Syatems," *Computer Methods in Applied Mechanics and Engineering*, vol. 1, pp. 1–16, 1972.

[2] K. E. Brenan, S. L. Campbell, and L. R. Petzold, *The Numerical Solution of Intial Value Problems in Differentail-Algebraic Equations*. Elsevier, New York, NY, 1989.

[3] D. Constantinescu, S. Salcudean, and E. Croft, "Haptic Rendering of Rigid Contacts using Impulsive and Penalty Forces," *IEEE Transactions on Robotics*, vol. 21, no. 3, pp. 309–323, 2005.

[4] D. Constantinescu, S. Salcudean, and E. Croft, "Local Models of Interaction for Realistic manipulation of Rigid Virtual Worlds," *The International Journal of Robotics Research*, vol. 24, no. 10, pp. 789–804, 2005.

[5] D. Constantinescu, S. Salcudean, and E. Croft, "Haptic Manipulation of Serial-Chain Virtual Mechanisms," *ASME Transactions Journal of Dynamic Systems, Measurement and Control*, vol. 128, no. 1, pp. 65–74, 2006.

[6] R. Featherstone, *Robot Dynamics Algorithms*. Boston:Kluwer, 1987.

[7] R. Featherstone, "Efficient Factorization of the Joint-Space Inertia Matri for Branched Kinematic Trees," *The International Journal of Robotics Research*, vol. 24, no. 9, pp. 487–500, 2005.

[8] R. Featherstone and O. Khatib, "Load Independence of the Dynamically Consistent Inverse of the Jacobian Matrix," *The International Journal of Robotics Research*, vol. 16, no. 2, pp. 168–170, 1997.

[9] J. Garcia de Jalon and E. Bayo, *Kinematics and Dynamics Simulation of Multibody Systems: The Real-Time Challenge*. Springer-Verlag, 1993.

[10] R. Gillespie, "Kane's Equations for Haptic Display of Multibody Systems," *Haptics-e*, vol. 3, no. 2, pp. 1–20, 2003.

[11] R. Gillespie, "On-Line Symbolic Constraint Embedding for Simulation of Hybrid Dynamical Systems," *Multibody Dynamics*, vol. 14, pp. 387–417, 2005.

[12] D. Lawrence, "Stability and Transparency in Bilateral Teleoperation," *IEEE Transactions on Robotics and Automation*, vol. 9, no. 5, pp. 624–637, 1993.

[13] P. Mitra and G. Niemeyer, "Dynamic Proxy Objects in Haptic Simulations," in *Proceedings of the IEEE Conference on Robotics, Automation and Mechatronics*, 2004, pp. 1054–1059.

[14] A. Nahvi, D. Nelson, J. Hollerbach, and D. Johnson, "Haptic Manipulation of Virtual Mechanisms from Mechanical CAD Designs," in *Proceedings of the IEEE International Conference on Robotics and Automation*, Leueven, Belgium, May 1998, pp. 375–380.

[15] P. E. Nikravesh, *Computer-Aided Analysis of Mechanical Systems*. Prentice-Hall, Englewood Cliffs, NJ, 1988.

[16] P. E. Nikravesh, "Systematic Reduction of Multibody Equations of Motion to a Minimal Set," *International Journal of Non-Linear Mechanics*, vol. 25, no. 2/3, pp. 143–151, 1990.

[17] D. Ruspini and O. Khatib, "Dynamic Models for Haptic Rendering Systems," in *Advances in Robot Kinematics: ARK98*, Strobl/Salzburg, Austria, 1998, pp. 523–532.

[18] D. Ruspini and O. Khatib, "Collision/Contact Models for Dynamic Simulation and Haptic Interaction," in *Proceedings of the International Symposium on Robotics Research*, Snowbird, UT, 1999, pp. 185–195.

[19] D. Ruspini and O. Khatib, "Haptic Display for Human Interaction with Virtual Dynamic Environments," *Journal of Robotic Systems*, vol. 18, no. 2, pp. 769–783, 2001.